

# Functional Alterations to the Nigrostriatal System in Mice Lacking All Three Members of the Synuclein Family

Sabina Anwar,<sup>2\*</sup> Owen Peters,<sup>1\*</sup> Steven Millership,<sup>1\*</sup> Natalia Ninkina,<sup>1,4</sup> Natalie Doig,<sup>5</sup> Natalie Connor-Robson,<sup>1</sup> Sarah Threlfell,<sup>2</sup> Gurdeep Kooner,<sup>1</sup> Robert M. Deacon,<sup>3</sup> David M. Bannerman,<sup>3</sup> J. Paul Bolam,<sup>5</sup> Sreeganga S. Chandra,<sup>6</sup> Stephanie J. Cragg,<sup>2</sup> Richard Wade-Martins,<sup>2</sup> and Vladimir L. Buchman<sup>1</sup>

<sup>1</sup>School of Biosciences, Cardiff University, Cardiff CF10 3AX, United Kingdom, <sup>2</sup>Department of Physiology, Anatomy and Genetics, <sup>3</sup>Department of Experimental Psychology, and Oxford Parkinson's Disease Centre, University of Oxford, Oxford OX1 3QX, United Kingdom, <sup>4</sup>Institute of Physiologically Active Compounds, Russian Academy of Sciences, Chernogolovka 142432, Moscow Region, Russian Federation, <sup>5</sup>Medical Research Council Anatomical Neuropharmacology Unit, Department of Pharmacology, and Oxford Parkinson's Disease Centre, University of Oxford, Oxford OX1 3TH, United Kingdom, and <sup>6</sup>Program in Cellular Neuroscience, Neurodegeneration and Repair, Department of Neurology, Department of Molecular Cellular and Developmental Biology, Yale University, New Haven, Connecticut 06536

The synucleins ( $\alpha$ ,  $\beta$ , and  $\gamma$ ) are highly homologous proteins thought to play a role in regulating neurotransmission and are found abundantly in presynaptic terminals. To overcome functional overlap between synuclein proteins and to understand their role in presynaptic signaling from mesostriatal dopaminergic neurons, we produced mice lacking all three members of the synuclein family. The effect on the mesostriatal system was assessed in adult (4- to 14-month-old) animals using a combination of behavioral, biochemical, histological, and electrochemical techniques. Adult triple-synuclein-null (TKO) mice displayed no overt phenotype and no change in the number of midbrain dopaminergic neurons. TKO mice were hyperactive in novel environments and exhibited elevated evoked release of dopamine in the striatum detected with fast-scan cyclic voltammetry. Elevated dopamine release was specific to the dorsal not ventral striatum and was accompanied by a decrease of dopamine tissue content. We confirmed a normal synaptic ultrastructure and a normal abundance of SNARE (soluble *N*-ethylmaleimide-sensitive factor attachment protein receptor) protein complexes in the dorsal striatum. Treatment of TKO animals with drugs affecting dopamine metabolism revealed normal rate of synthesis, enhanced turnover, and reduced presynaptic striatal dopamine stores. Our data uniquely reveal the importance of the synuclein proteins in regulating neurotransmitter release from specific populations of midbrain dopamine neurons through mechanisms that differ from those reported in other neurons. The finding that the complete loss of synucleins leads to changes in dopamine handling by presynaptic terminals specifically in those regions preferentially vulnerable in Parkinson's disease may ultimately inform on the selectivity of the disease process.

## Introduction

$\alpha$ -Synuclein is central to the etiology of Parkinson's disease (PD), a neurodegenerative condition in which dopaminergic neurons projecting from the substantia nigra pars compacta (SNpc) to the dorsal striatum are particularly vulnerable (Goedert, 2001; Trojanowski and Lee, 2002).  $\alpha$ -Synuclein has long been associated

with PD neuropathology and the familial forms of the disease, and more recent genome-wide association studies implicate variation in  $\alpha$ -synuclein as an etiological factor in idiopathic forms of PD and other synucleinopathies (Mizuta et al., 2008; Pankratz et al., 2009; Satake et al., 2009; Scholz et al., 2009; Simón-Sánchez et al., 2009).

Given this strong association with disease, it is essential that we understand the roles of  $\alpha$ -synuclein in the normal function of dopaminergic neurons to learn how  $\alpha$ -synuclein dysfunction contributes to neurodegeneration.  $\alpha$ -Synuclein has been shown to play a role in many processes important to synaptic dopamine turnover (for review, see Venda et al., 2010). Much of the experimental evidence has, however, been obtained *in vitro* or in cultured cells (Jenco et al., 1998; Perez et al., 2002; Wersinger and Sidhu, 2003; Peng et al., 2005; Larsen et al., 2006; Tehrani et al., 2006; Fountaine et al., 2008; Liu et al., 2008), and similar roles have yet to be identified in the adult brain where normal connectivity is preserved. Moreover, studies of neurotransmitter release in knock-out (KO) and transgenic mice or primary neurons obtained from these animals have produced conflicting data about the role of normal or mutated  $\alpha$ -synuclein (Abeliovich et al., 2000; Cabin et al., 2002; Chandra et al., 2004; Liu et al., 2004;

Received Nov. 28, 2010; revised Feb. 21, 2011; accepted March 1, 2011.

Author contributions: S.J.C., R.W.-M., and V.L.B. designed research; S.A., O.P., S.M., N.N., N.D., N.C.-R., S.T., G.K., and V.L.B. performed research; S.S.C. contributed unpublished reagents/analytic tools; N.N., R.D., D.M.B., J.P.B., S.S.C., S.J.C., R.W.-M., and V.L.B. analyzed data; S.J.C., R.W.-M., and V.L.B. wrote the paper.

This work was supported by Wellcome Trust Programme Grant 075615/Z/04/z (V.L.B.), a New Investigator Award from Research into Ageing (R.W.-M.), and National Institutes of Health Grant R01 NS064963 (S.S.C.). S.A. and N.C.-R. were supported by studentships from the Medical Research Council, S.T. was supported by Parkinson's United Kingdom, and D.M.B. is a Wellcome Trust Senior Research Fellow. We are grateful to Thomas C. Südhof for sharing with us  $\beta$ -synuclein-KO mice and commenting on this manuscript.

The authors declare no competing financial interests.

\*S.A., O.P., and S.M. contributed equally to this work.

Correspondence should be addressed to one of the following: Vladimir L. Buchman, School of Biosciences, Cardiff University, Cardiff CF10 3AX, UK, E-mail: buchmanvl@cf.ac.uk; or Richard Wade-Martins or Stephanie J. Cragg, Department of Physiology, Anatomy, and Genetics, University of Oxford, Oxford OX1 3QX, UK, E-mail: richard.wade-martins@dpag.ox.ac.uk or stephanie.cragg@dpag.ox.ac.uk.

DOI:10.1523/JNEUROSCI.6194-10.2011

Copyright © 2011 the authors 0270-6474/11/317264-11\$15.00/0

Yavich et al., 2004, 2005; Unger et al., 2006; Senior et al., 2008; Garcia-Reitböck et al., 2010; Nemani et al., 2010; Scott et al., 2010).

The high level of similarity in amino acid sequence, overlapping expression patterns, and abundance of all three synucleins in presynaptic terminals suggest the potential for functional overlap. Compensatory function is supported by increased expression of the remaining family member in the CNS of  $\alpha/\gamma$ -synuclein and  $\alpha/\beta$ -synuclein double-KO mice (Chandra et al., 2004; Robertson et al., 2004). Moreover, development of pathology in cysteine string protein (CSP $\alpha$ )-KO mice is accelerated in the absence of both  $\alpha$ - and  $\beta$ -synuclein to a greater extent than in the absence of either alone (Chandra et al., 2005), further arguing for overlapping function of synuclein family members.

To better understand the role of the synucleins in dopamine neurotransmission and to overcome compensatory changes and functional overlap, we produced synuclein-free mice and studied the outcome on the function of mesostriatal neurons. In the nigrostriatal system of triple-synuclein-null (TKO) mice, we reveal substantial changes in synaptic dopamine neurotransmission, but no overt structural alterations in the dopaminergic neurons or their synapses. Moreover, we identify that the effect of depletion of all synucleins on dopamine transmission is specific to the dorsal but not ventral striatum, which correlates with the regional vulnerability in PD. Our data point to the unique importance of the synucleins to the nigrostriatal system, consistent with association of  $\alpha$ -synuclein to PD.

## Materials and Methods

### Generation of double- and triple-synuclein-null mutant animals

Generation of  $\alpha/\gamma$ -synuclein double-KO mice on C57BL/6J (Charles River) background was described previously (Robertson et al., 2004). Heterozygous  $\beta$ -synuclein-KO mice (Chandra et al., 2004) on C57BL/6J background were further backcrossed with C57BL/6J (Charles River) mice for six generations in Cardiff University Transgenic Animal Unit before breeding with  $\alpha/\gamma$ -synuclein double-KO mice. Resultant triple-heterozygous animals were intercrossed to produce founders of triple-KO and wild-type colonies used in this study. Thus, all studied animals were on the same C57BL/6J genetic background. If not stated otherwise, 4- to 5-month-old male mice were used in experiments. Investigators who performed behavioral and postmortem analyses were blinded with respect to the sample genotype. All animal work was performed in accordance with the United Kingdom Animals (Scientific Procedures) Act (1986).

### Behavioral analyses

Balance and coordination of experimental animals were analyzed using static rods and accelerating rotarod tests. Locomotor activity was measured in the home cage or nonanxiogenic open field. Spontaneous alternation in a T-maze, elevated plus maze, holeboard, and bright open-field tests were used to assess animal anxiety and exploratory behavior. The above methods were described in our previous publications (Robertson et al., 2004; Senior et al., 2008).

**Inverted grid test.** Mice were placed onto a 30 × 30 cm square mesh consisting of 5 mm squares of 0.5-mm-diameter wire. The grid was slowly rotated to the inverted position and held above a thick layer of bedding material. If a mouse fell from the grid earlier than the maximum test time of 1 min, the latency to fall was noted and after a 10 min rest in the home cage, the test was repeated. The best result from three attempts was included in the statistics.

**Activity camera.** Animals were moved to the testing room 30 min before the start of the test. The lighting in the test room was the same as in the animal holding room. Each animal was placed in an individual transparent 40 × 40 cm Perspex box equipped with a system of infrared beams to monitor activity (Ugo Basile). Data (number of beam breaks) were collected at 4 min intervals for 2 h.

**Climbing test.** Animals injected with 4 mg/kg apomorphine were placed in 12-cm-diameter cylindrical individual cages with walls of vertical, 2-mm-diameter, 1-cm-apart metal bars as described previously (Protais et al., 1976) and filmed for 90 min. Climbing was scored constantly and expressed as the number of seconds within each 4 min interval that an animal spent with forefeet holding the cage wall bars plus double the number of seconds when all four paws were holding the wall bars.

### Pharmacological treatments

All drug solutions for injections were freshly prepared. 3-Hydroxybenzylhydrazine (NSD-1015), methyl L-3,4-dihydroxyphenylalanine (L-DOPA), cocaine, and D-amphetamine (dAMPH) (all from Sigma-Aldrich) were dissolved in sterile 0.9% saline and apomorphine in sterile 0.1% ascorbic acid/0.9% saline. Five or 10 ml/kg of a drug solution or vehicle were injected intraperitoneally or subcutaneously as indicated.

**Cocaine and amphetamine.** Thirty minutes after placement in the activity camera, animals received a single intraperitoneal injection of 10 mg/kg cocaine or 4 mg/kg D-amphetamine and were immediately returned into the same camera for an additional 90 min of activity recording.

**L-DOPA.** After accommodation in the testing room for 20 min, animals received a single intraperitoneal injection of 50 mg/kg methyl L-DOPA hydrochloride and were returned to the home cage. Twenty minutes after injection, animals were placed into the activity camera for activity testing and amphetamine injections that were performed exactly as described above.

**Apomorphine.** For subcutaneous injections, apomorphine was dissolved at a concentration of 0.4 mg/ml. Animals that received 4 mg/kg apomorphine were analyzed for climbing behavior as described above.

**NSD-1015.** To measure the *in vivo* rate of dopamine biosynthesis, mice were injected intraperitoneally with 100 mg/kg NSD-1015 (Carlsson et al., 1972). The dorsal striata were dissected from animals killed 40 min after the injection, and the level of accumulated L-DOPA was determined by HPLC analysis as described below.

### Biochemical analysis

Protein extraction and Western blotting were performed as described in our previous publications (Buchman et al., 1998; Robertson et al., 2004; Al-Wandi et al., 2010). Coimmunoprecipitation of soluble N-ethylmaleimide-sensitive factor attachment protein receptor (SNARE) proteins was performed as described previously (Burré et al., 2010). Primary antibodies and dilutions are listed in a table (see Notes). For detection of protein bands on Western blots, fluorescently labeled (Cy3 or Cy5) secondary antibodies and the FluorChem Q MultiImage III system (Alpha Innotech) were used. Band intensities were quantified using FluorChem Q, version 1.3.0, analysis software. Relative concentrations of each protein in analyzed samples were calculated after normalizing band intensities against intensities of housekeeping protein ( $\beta$ -actin,  $\alpha$ -tubulin, or GAPDH) bands.

Monoamines were measured by HPLC with electrochemical detection as described previously (Senior et al., 2008; Al-Wandi et al., 2010) using a 4.6 × 150 mm Microsorb C18 reverse-phase column (Varian) and Decade II ECD with a Glassy carbon working electrode (Antec Leyden) set at +0.7 V with respect to a Ag/AgCl reference electrode. For measuring dopamine and its metabolites, the mobile phase consisted of 12% methanol (v/v), 0.1 M monosodium phosphate, 2.4 mM 1-octane sulfonic acid (OSA), 0.68 mM EDTA, pH 3.1. For L-DOPA, a mobile phase of the same composition but containing 0.4 mM OSA was used.

### Immunohistochemistry and neuronal cell counts

Fixation, processing, embedding, preparing of microtome sections, and their immunostaining were performed as in our previous studies (Buchman et al., 1998; Robertson et al., 2004; Ninkina et al., 2009; Al-Wandi et al., 2010). Primary antibodies and dilutions are listed in a table (see Notes). Stereological counting of neurons was performed as previously described for single- and double-synuclein-KO mice (Ninkina et al., 2003; Robertson et al., 2004; Al-Wandi et al., 2010).

### Fast-scan cyclic voltammetry

Ten- to 14-month-old mice were killed by cervical dislocation and decapitated, and their brains were removed over ice. Three hundred fifty micrometer coronal striatal slices were cut using a vibratome (Leica Microsystems) in ice-cold HEPES-buffered physiological saline saturated with 95% O<sub>2</sub>/5% CO<sub>2</sub> and maintained in a bicarbonate-buffered artificial CSF (containing 2.4 mM Ca<sup>2+</sup>) as described previously (Cragg, 2003; Rice and Cragg, 2004). Extracellular dopamine concentration was monitored and quantified in the dorsal and ventral striatum at 32°C using fast-scan cyclic voltammetry (FCV) as previously described (Cragg, 2003) with 10- $\mu$ m-diameter carbon-fiber microelectrodes (exposed tip length, ~50–100  $\mu$ m, fabricated in-house) and a Millar voltammeter (Julian Millar, Barts and The London School of Medicine and Dentistry, London, UK). The applied voltage was a triangular waveform, with a voltage range of -0.7 to 1.3 to -0.7 V versus Ag/AgCl at a scan rate of 800 V/s. The sampling frequency was 8 Hz. Data were acquired and analyzed using Strathclyde Whole Cell Program (University of Strathclyde, Glasgow, UK). Electrodes were positioned in striatal slices to a depth of 100  $\mu$ m. The evoked current signal was confirmed as dopamine by comparing the potentials for peak oxidation and reduction currents with those of dopamine in calibration media (+500–600 and -200 mV vs Ag/AgCl, respectively). Electrodes were calibrated in 1–2  $\mu$ M dopamine in experimental media. Dopamine release was evoked by a surface, concentric bipolar Pt/Ir electrode (25  $\mu$ m diameter; FHC) as described previously (Rice and Cragg, 2004). Stimulus pulses generated out-of-phase with FCV scans and were applied at the lowest current that generated maximal dopamine release with a single stimulus pulse in wild-type animals (650  $\mu$ A, 200  $\mu$ s pulse duration).

FCV experiments assessed extracellular dopamine concentration ([DA]<sub>o</sub>) evoked by discrete stimuli in the caudate–putamen (CPU) and nucleus accumbens (NAc). Recording sites classed as CPU were located dorsal to the anterior commissure (AC); NAc was ventral to the AC.

Data were collected through one of two experimental designs. First, several sites were sampled per slice (six to eight CPU, four NAc) in both genotypes on the same experimental day. Stimuli in these experiments consisted of either a single pulse or burst pulses (four pulses at 100 Hz). In the second stimulation paradigm, recordings were taken at a single recording site at 2.5 min intervals, to ensure consistent release, and consisted of either single pulses or trains of five pulses at a range of frequencies (1–100 Hz) in randomized order. These frequencies span the full range of dopaminergic neuron firing frequencies reported *in vivo*. For these experiments in CPU, recording sites were in the dorsal half of the nucleus. Data are means  $\pm$  SEM, and the sample size, *n*, is the number of observations. The number of animals in each data set was >3. Comparisons for differences in means were assessed by one-way ANOVA and *post hoc* Bonferroni's multiple-comparison *t* test or unpaired *t* test using GraphPad Prism.

Dopamine uptake was assessed by comparing the decay phases of dopamine transients evoked by a single pulse between the two genotypes. Dopamine transients were concentration matched for a peak of  $1.0 \pm 0.1$   $\mu$ M from five animals in each genotype. Dopamine uptake via dopamine active transporter (DAT) is the principal factor governing dopamine decay in these evoked transients (Giros et al., 1996). The rate of dopamine uptake by the DAT obeys Michaelis–Menton kinetics and is therefore proportional to  $V_{\max}$  and varies with [DA]<sub>o</sub>. Comparison of the decay phase of dopamine transients matched for similar peak [DA]<sub>o</sub> eliminates differences in uptake rate caused by differences in [DA]<sub>o</sub>; therefore, prevailing differences in  $V_{\max}$  should be apparent (Cragg et al., 2000).

### Electron microscopy

**Sample preparation.** Mice were terminally anesthetized and perfuse-fixed with 4% paraformaldehyde and 0.1% glutaraldehyde. Sagittal vibratome sections (60  $\mu$ m) were incubated in a primary antibody against tyrosine hydroxylase (TH), and dopaminergic axons were revealed using either silver-intensified immunogold particles or a peroxidase reaction using diaminobenzidine (DAB) as the chromogen (Moss and Bolam, 2008). All sections were then washed three times in 0.1 M phosphate buffer (PB), pH 7.4. The sections were postfixed in 1% osmium tetroxide in PB (Oxkem)

for either 7 min (immunogold) or 40 min (DAB peroxidase). After washing in 0.1 M PB, sections were dehydrated in an ascending series of ethanol dilutions [15 min in 50% ethanol, 35 min in 70% ethanol, which included 1% uranyl acetate (TAAB), 15 min in 95% ethanol, and twice 15 min in absolute ethanol]. After absolute ethanol, sections were washed twice in propylene oxide (Sigma-Aldrich) for 15 min, placed into resin (Durcupan ACM; Fluka), and left overnight (~15 h) at room temperature. The resin was then warmed to reduce its viscosity, and sections were placed on microscope slides, a coverslip applied, and the resin cured at 65°C for ~70 h.

**Electron-microscopic analysis.** All sections were examined in the light microscope and areas from the dorsolateral striatum were cut from the slide, glued to the top of a resin block, and trimmed with razor blades. Serial sections, ~50 nm thick (gray/silver), were cut using an ultramicrotome (Leica EM UC6; Leica Microsystems), collected on pioloform-coated, single-slot copper grids (Agar Scientific), and lead-stained to improve contrast for electron-microscopic examination. A Philips CM10 electron microscope was used to examine the sections. Analyses of preembedding immunogold sections were performed at a minimum of 5  $\mu$ m from the tissue–resin border (i.e., the surface of the section). The maximum distance from the tissue–resin border examined was determined by the penetration of the gold conjugated antibody together with the angle at which the tissue–resin was sectioned, and was therefore variable.

For both immunogold and peroxidase-labeled tissue, TH-positive structures were systematically analyzed in one of the serial sections on an electron-microscopic grid. At a magnification at which it is not possible to clearly visualize synapses (1950 $\times$ ), an area was chosen at random, the magnification was then increased (25,000 $\times$ ), and the first structure positively labeled for TH was digitally recorded at an indicated magnification of 36,500 $\times$  (Gatan multiscan CCD camera; Gatan). TH-positive structures were identified and imaged, in this way, continuing systematically in straight lines across the section, keeping the identified TH-positive structure central within the image frame. For immunogold-labeled structures, the criterion for an immunopositive structure was five or more silver-intensified immunogold particles. This systematic process was continued within the same section until 25 TH-positive structures were identified and imaged, the process was then repeated using a different section on a different grid until 50 TH-immunopositive structures were identified and imaged per animal for both immunogold labeled tissue (150 images in total) and peroxidase-labeled tissue (150 images in total). Symmetric synapses (Gray's type II) were identified by the presence of presynaptic and postsynaptic membrane specializations, a widened synaptic cleft and cleft material. Any structures seen to be forming such symmetric synapses were imaged at a higher magnification of 46,500 $\times$ .

**Quantitative EM image analysis.** Digital images were analyzed using the publicly available software ImageJ (<http://rsbweb.nih.gov/ij/>) and the ImageJ plug-ins PointDensity and PointDensitySyn (<http://folk.uio.no/maxdl/software.html>) (Larsson and Broman, 2005). Images were adjusted for contrast and brightness using Adobe Illustrator and Photoshop (version CS3; Adobe Systems).

For analysis of TH-positive (peroxidase-labeled) structures, the central TH-positive structure within the image frame was analyzed by tracing the perimeter, the number of mitochondria within the profile was counted, and if the structure was forming a synaptic specialization, then the length of the active zone(s) was measured. The active zone was defined as the length of plasma membrane opposing the postsynaptic density, across the synaptic cleft. Other TH-positive structures completely within the electron micrograph frame were counted. Analysis of immunogold-labeled TH-positive structures was performed using PointDensity, the perimeter of the central structure within the frame was delineated, and then a point marker was placed within the center of each vesicle. Vesicles were marked if at least 50% of the vesicle membrane was visible. All other TH-positive profiles within the frame were counted. TH-positive profiles that were forming synapses were analyzed using PointDensitySyn, the plasma membrane of the structure was traced, the active zone(s) were delineated, and points were placed in the center of the vesicles.

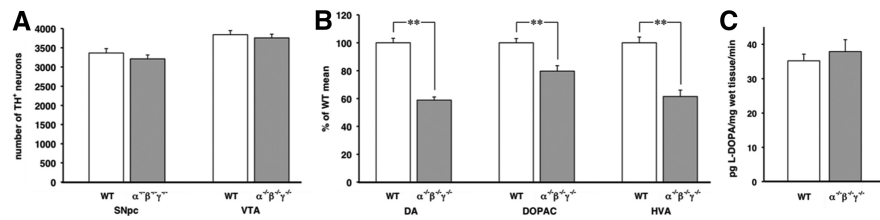


**Figure 1.** Triple-synuclein-null mutant mice possess a normal complement of dopaminergic neurons in the SNpc and VTA, normal rate of *in vivo* TH activity, but reduced level of dopamine and its metabolites in the striatum. **A**, The bar charts show means  $\pm$  SEM of total number of TH-positive neurons in SNpc and VTA of 4-month-old wild-type (WT) ( $n = 18$ ) and TKO ( $\alpha^{-/-}\beta^{-/-}\gamma^{-/-}$ ) ( $n = 28$ ) mice. Neurons were stereologically counted separately in the left and right structures. **B**, Striatal concentrations (picomoles per milligram of protein) of dopamine (DA) and its metabolites, DOPAC and HVA, were normalized to the mean value for wild-type animals (100%). Means  $\pm$  SEM of data obtained from 15 wild-type (WT) and 14 TKO ( $\alpha^{-/-}\beta^{-/-}\gamma^{-/-}$ ) mouse samples are shown (\*\* $p < 0.01$ ; Kolmogorov–Smirnov test). For metabolite/dopamine ratios, see table (see Notes). **C**, The rate of L-DOPA accumulation in the striatum of wild-type (WT) ( $n = 5$ ) and TKO mice ( $\alpha^{-/-}\beta^{-/-}\gamma^{-/-}$ ) ( $n = 5$ ) after intraperitoneal injection of 100 mg/kg AADC inhibitor NSD-1015.

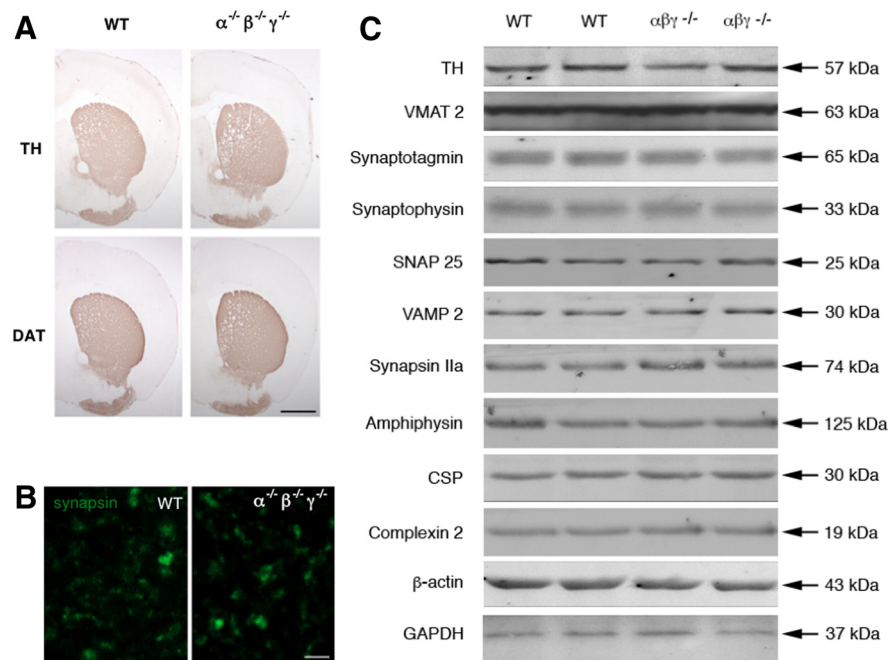


**Figure 2.** Normal morphology and expression of synaptic markers in the striatum of triple-synuclein-null mutant mice. **A**, TH and DAT expression in the striatum of 4-month-old mice. Representative microphotographs of coronal sections of wild-type (WT) and TKO ( $\alpha^{-/-}\beta^{-/-}\gamma^{-/-}$ ) mouse brains at the bregma 0.38 mm level. Scale bar, 1 mm (for all images). **B**, High-magnification confocal images of striatal sections immunofluorescently stained with antibodies against synapsin IIa. Scale bar, 2  $\mu$ m (for both images). **C**, Western blot analysis of proteins in the striatum of wild-type and mutant mice. Representative Western blots show analysis of striatal samples from two mice for each genotype.

### Statistical analysis

All data are presented as means  $\pm$  SEM. Statistical analysis was performed using SPSS/PASW Statistics, versions 16.0 or 18.0 (SPSS), GraphPad Prism 4.0 (GraphPad Software), and GB-Stat PPC 6.5.4 (Dynamic Microsystems).

## Results

### Generation of TKO mice

At all stages of the breeding program (see Materials and Methods), an expected Mendelian frequency of TKO mice on pure C57BL/6J genetic background was observed in weaned litters. TKO mice, studied up to 14 months of age, were phenotypically indistinguishable from wild-type mice generated within the same breeding program and no differences in size, weight, or gross anatomy of the brain of TKO and wild-type mice were observed.

Because of the well known links between  $\alpha$ -synuclein and dopamine dysfunction in Parkinson's disease, and the prominent expression and presynaptic localization of all three synuclein family members in dopaminergic neurons of the SNpc [data are available (see Notes)] (Abeliovich et al., 2000), we performed in-depth studies on the midbrain dopaminergic systems of TKO mice.

### Normal numbers of dopaminergic neurons in the SNpc and normal expression of synaptic markers in the striatum of TKO mice

Stereological counts of midbrain dopaminergic neurons, identified by immunostaining for TH, revealed no difference in the number of neurons in the SNpc and ventral tegmental area (VTA) of TKO mice compared with wild-type mice (Fig. 1A). Immunostaining of the striatum with markers of dopaminergic terminals, TH or DAT (Fig. 2A), or general synaptic marker synapsin IIa (Fig. 2B), and quantitative Western blot analysis of striatal tissue proteins (Fig. 2C) [quantification of data is available (see Notes)] also revealed no differences in morphology or levels of all studied synaptic markers.

### Decreased levels of dopamine and its metabolites in the striatum of TKO mice

HPLC analysis of tissue monoamines revealed that the dopamine content in the dorsal striatum of 4-month-old male TKO mice was substantially decreased compared with wild-type animals (Fig. 1B). The levels of the major dopamine metabolites, 3,4-dihydroxyphenylacetic acid (DOPAC) and homovanillic acid (HVA), were less affected, resulting in increases of DOPAC/dopamine and HVA/dopamine ratios (Fig. 1B) [additional data are available (see Notes)]. To determine whether decreased striatal dopamine level in mutant mice is a

consequence of reduced activity of TH, the rate-limiting enzyme in dopamine synthesis, we inhibited aromatic L-amino acid decarboxylase (AADC), the enzyme immediately downstream of TH in the synthetic pathway, by treating mice with NSD-1015. Striatal extracts were prepared 45 min after intraperitoneal injection of 100 mg/kg of the inhibitor, and the level of L-DOPA was assessed by HPLC. No difference in L-DOPA accumulation, which is an indicator of *in vivo* TH activity, was found between wild-type and TKO mice (Fig. 1C). Together, these data suggest that, in the absence of neuronal loss or obvious biochemical or morphological changes of dopaminergic synapses [also confirmed by electron microscopy analysis (see below)], TKO mice display signs of synaptic dysfunction in the nigrostriatal system at the level of regulation of dopamine availability. Therefore, we studied performance of TKO mice in behavior tests, the results of

which might be affected by alterations in dopamine neurotransmission.

### Hyperdopaminergic-like behavior of TKO mice

The inverted grid and static rods tests were used to assess balance and coordination of 4-month-old TKO mice. The performance of both male and female adult mutant mice was very similar to the performance of age/gender-matched wild-type mice (Fig. 3A) [additional data are available (see Notes)]. However, aging mutant mice gradually lose the ability to stay on the inverted grid (Fig. 3A). In contrast, the accelerated rotarod test, in which the animal's endurance capacity affects the results, revealed significantly compromised performance of TKO mice already at the age of 4 months (Fig. 3B).

Wild-type and TKO animals behaved in a similar manner in the bright open-field and elevated plus maze tests [data are available (see Notes)], suggesting that the lack of synucleins does not affect mouse anxiety.

Several tests revealed significant differences in the activity in novel nonanxiogenic environment and exploratory behavior of wild-type and TKO mice. In the nonanxiogenic open field, mutant mice were more active (Fig. 3D) and reared more often (Fig. 3E). In the hole-board test, the number of nose pokes into holes was significantly greater for mutant than wild-type mice (Fig. 3F, G), suggesting increased overall exploratory behavior. TKO mice also showed a trend toward a decreased spontaneous alternation in a T-maze (Fig. 3C). Finally, monitoring of animal activity in the home-like cage demonstrated that TKO mice respond to changes in the environment with a substantially greater increase in locomotion than wild-type mice (Fig. 3H). However, after adaptation to the new environment, the locomotor activity of mice was similar for both genotypes (Fig. 3I).

### Increased levels of electrically evoked dopamine in the dorsal striatum of TKO mice

Together, these data suggest that, despite a decrease in striatal dopamine levels, TKO mice exhibit behavior typical of hyperdopaminergic animals (Zhuang et al., 2001), suggesting that synaptic mechanisms regulating dopamine release or uptake might be modified in the absence of synucleins. We used FCV at carbon-fiber microelectrodes to assess subsecond release and uptake of dopamine in the dorsal (CPu) and ventral (NAc) striatum.

In the CPu, mean peak extracellular concentrations of dopamine ( $[DA]_o$ ) evoked by single pulses or burst stimuli (four pulses, 100 Hz) across a large number of recording sites were  $\sim 1.5$ -fold greater in TKO than wild-type mice (Fig. 4A, B) [additional data are available (see Notes)]. By contrast, in the NAc no difference in evoked  $[DA]_o$  was detected between the two genotypes (Fig. 4D) [additional data

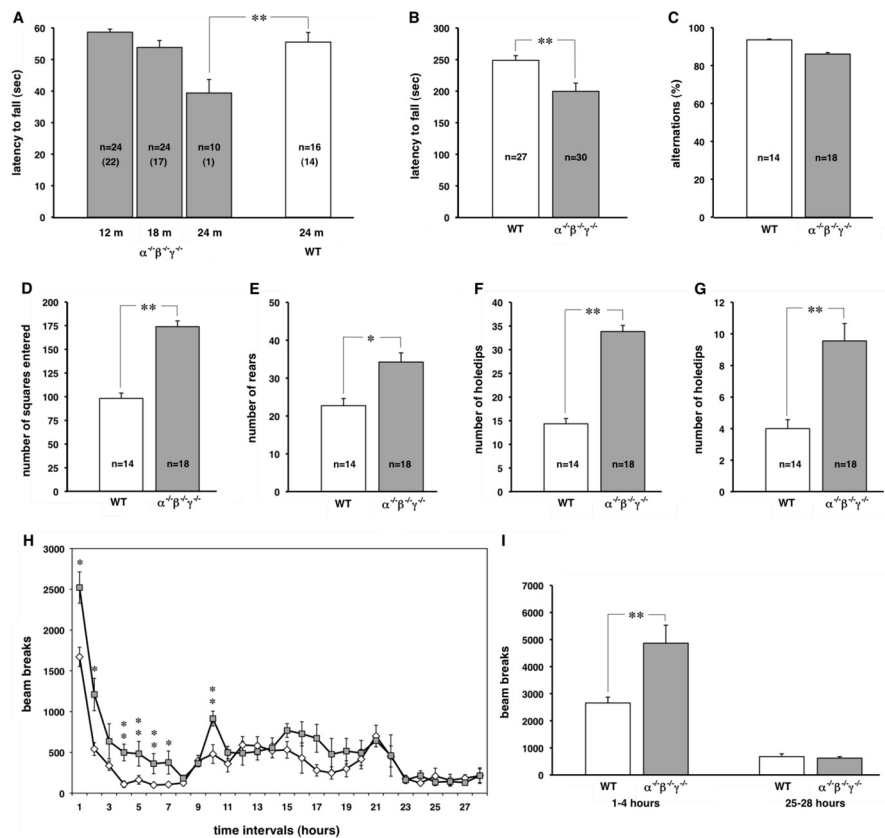


**Figure 3.** Performance of wild-type and triple-synuclein-null mutant mice in balance/coordination and exploratory behavior tests and their activity in novel nonanxiogenic environment. The bar charts show means  $\pm$  SEM of experimental values obtained by testing wild-type (WT) and TKO ( $\alpha^{-/-}\beta^{-/-}\gamma^{-/-}$ ) mice. For all panels, the number of animals tested and, where appropriate, a statistically significant difference are shown (\* $p < 0.05$ ; \*\* $p < 0.01$ ; Kolmogorov–Smirnov test). **A**, The latency to fall from the inverted grid of male 2-year-old wild-type and mutant mice of various ages. The number of animals that successfully completed the task at least once from three attempts is shown for each experimental group (in brackets). The best result for each mouse was used for calculating the group mean. **B**, The latency to fall from the accelerating rotarod of 4-month-old male mice. **C**, Percentage of trials in which 4-month-old female mice alternated in a T-maze. The difference between groups reached significance ( $p = 0.037$ ) only when less robust Mann–Whitney test but not Kolmogorov–Smirnov test was used. The number of squares 4-month-old female mice entered (**D**) and the number of rears (**E**) during 3 min testing in nonanxiogenic open field. The number of nose pokes into peripheral (**F**) and central (**G**) holes during 3 min assessing of 4-month-old female mice in the hole-board test. **H**, **I**, The locomotor activity (number of infrared beam breaks) of 4-month-old male wild-type (white diamonds;  $n = 13$ ) and mutant (gray squares;  $n = 13$ ) mice in a home-like cage monitored for 28 h. Total number of breaks for each 1 h interval (**H**) and for the first or last 4 h intervals (**I**), both corresponding to 10:00 A.M. to 2:00 P.M., are shown. Note that a sharp increase of animal activity during the 10th interval was triggered by switching off the room light.

are available (see Notes)]. The frequency dependence of dopamine release at given recording sites assessed across a full range of frequencies observed for dopaminergic neurons *in vivo* (1–100 Hz) was similar in both genotypes (Fig. 4C) [additional data are available (see Notes)] and consistent with previous observations in CPu and NAc (Exley et al., 2008). Analysis by HPLC of dopamine content in CPu and NAc subdissected from slices used for FCV confirmed that dopamine content in CPu was  $\sim 30\%$  lower in triple-synuclein-null mice (Fig. 4E; as seen in fresh tissue, Fig. 1B) and identified that, in the NAc, dopamine content was not different between genotypes (Fig. 4F).

### Increased evoked dopamine in the dorsal striatum is not attributable to differences in nicotinic receptor function or the $Ca^{2+}$ dependence of release

Since in CPu of TKO mice, dopamine content is two-thirds of wild type, but release is  $\sim 1.5$ -fold greater, deletion of all three synucleins results in a  $>2$ -fold increase in the releasability of the available dopamine. Because striatal acetylcholine (ACh) is a crit-

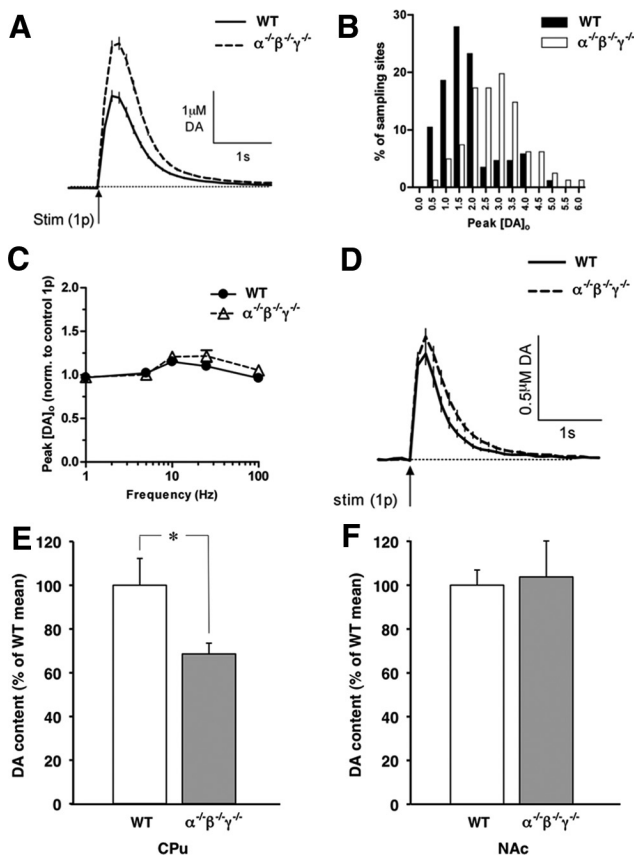


**Figure 4.** Electrically evoked dopamine transients and regulation of dopamine signals by firing frequency in wild-type and triple-synuclein-null mutant mice measured by FCV. **A**, Mean profiles of  $[DA]_0$  versus time (mean  $\pm$  SEM) after a single pulse ( $0.2 \mu\text{s}$ ; arrow) in the dorsal striatum (CPu). In CPu, peak  $[DA]_0$  transiently evoked by single pulses is greater in triple-synuclein-null mutant ( $\alpha^{-/-}\beta^{-/-}\gamma^{-/-}$ ) than wild-type (WT) mice [\*\*\* $p < 0.001$ , one-way ANOVA; WT,  $n = 81$ ;  $\alpha^{-/-}\beta^{-/-}\gamma^{-/-}$ ,  $n = 86$  (5 animals for each genotype)]. **B**, Histogram of peak  $[DA]_0$  of evoked dopamine transients in the CPu in wild-type versus triple-synuclein-null mutant mice for individual sampling sites. **C**, Mean peak  $[DA]_0 \pm$  SEM versus frequency during five-pulse trains (1–100 Hz) in the CPu in both genotypes ( $p > 0.05$ , two-way ANOVA; 3 animals per genotype). **D**, Mean profiles of  $[DA]_0$  versus time (mean  $\pm$  SEM) after a single pulse (arrow) in the ventral striatum (NAc). There is no significant difference between genotype in peak evoked  $[DA]_0$  [ $p > 0.05$ , one-way ANOVA;  $n = 26$  for both genotypes (4 animals per genotype)]. **E, F**, Dopamine concentrations (nanograms per milligram of protein) in the CPu and NAc dissected from the striatal slices were normalized to the mean value for wild-type animals in each brain structure (100%). Means  $\pm$  SEM of data obtained from 8 wild-type (WT) and 11 triple-synuclein-null mutant ( $\alpha^{-/-}\beta^{-/-}\gamma^{-/-}$ ) mouse samples are shown (\* $p < 0.05$ ; Kolmogorov–Smirnov test).

ical regulator of dopamine release probability, we assessed how dopaminergic synapses of TKO mice perform independently of ACh input. The nicotinic acetylcholine receptor (nAChR) antagonist dihydro- $\beta$ -erythroidine hydrobromide (DH $\beta$ E) modified evoked  $[DA]_0$  in a frequency-dependent manner (Fig. 5A, B), but similarly in both genotypes. Furthermore, in the absence of nAChR activity, the underlying range of  $[DA]_0$  released by four pulses (4p) at 100 Hz versus 1 Hz was an approximately threefold to fourfold range in both genotypes (Fig. 5A, B), consistent with a similar release probability in both genotypes. Therefore, the observed increase in dopamine releasability in CPu of triple-synuclein-null mice is not readily attributable to an upregulation of either nAChR function or underlying dopamine release probability.

We assessed whether the higher evoked  $[DA]_0$  despite reduced dopamine content in CPu of triple-synuclein-null mice may be

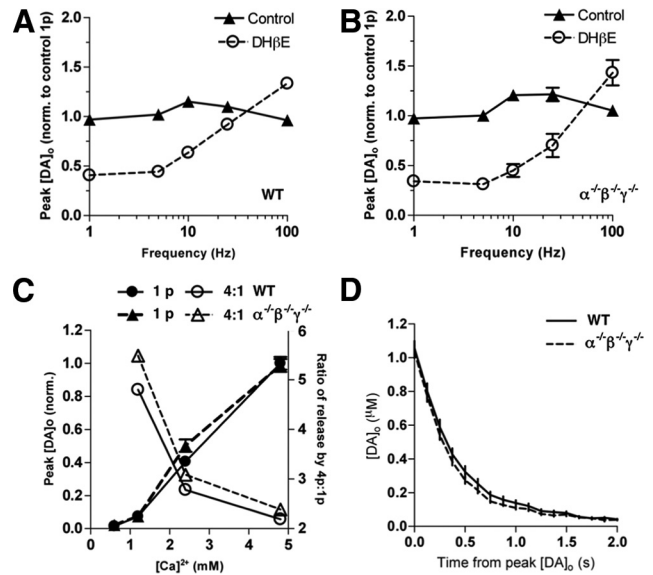


**Figure 5.** Regulation of dopamine signaling by cholinergic input, calcium, and uptake probability are similar in the CPu of wild-type and triple-synuclein-null mutant mice. **A, B**, Mean peak  $[DA]_0 \pm$  SEM versus frequency during five-pulse trains (1–100 Hz) in the dorsal striatum of wild-type (**A**) and TKO (**B**) mice, with and without inhibition of nAChRs (using DH $\beta$ E). Data are normalized to  $[DA]_0$  under control conditions (\*\*\* $p < 0.001$ , two-way ANOVA; 3 animals per genotype). **C**, Response of mean peak  $[DA]_0$  evoked by a single pulse to varying extracellular calcium concentrations (0.6–4.8 mM) in CPu (in the presence of DH $\beta$ E) did not significantly differ between genotypes ( $p > 0.05$ , two-way ANOVA; 4 animals per genotype). Data for each genotype are normalized to mean peak  $[DA]_0$  released at 4.8 mM  $\text{Ca}^{2+}$ . Ratio of release by a four-pulse burst (100 Hz) versus a single pulse (4p:1p, right hand y-axis) as a function of calcium concentration for both genotypes ( $p > 0.05$ , two-way ANOVA; 4 animals per genotype). **D**, Comparison of the rates of decay of concentration-matched dopamine transients suggests that dopamine uptake rates are not significantly different between the two genotypes ( $p > 0.05$ , two-way ANOVA;  $n = 8$  for wild-type and  $n = 7$  for mutant mice).

caused by a modified sensitivity of the exocytotic machinery to calcium. Varying extracellular calcium (in the presence of DH $\beta$ E to eliminate confounding effects on  $\text{Ca}^{2+}$ -dependent ACh release) modified  $[DA]_0$  evoked by a single pulse in both genotypes as predicted, but in a manner that was not significantly different (Fig. 5C). Furthermore, the ratio of  $[DA]_0$  evoked by a burst (4p/100 Hz) versus one pulse (4p:1p) decreased as expected with increasing  $[\text{Ca}^{2+}]_0$  but with no difference between genotypes (Fig. 5C), indicating no difference in the relative probability of dopamine release between genotypes.

#### Increased levels of evoked dopamine in the dorsal striatum is not attributable to differences in uptake of dopamine

Functional interactions between  $\alpha$ -synuclein and DAT have been suggested previously (Lee et al., 2001; Wersinger and Sidhu, 2003; Fountaine et al., 2008). Therefore, we investigated whether higher evoked  $[DA]_0$  in TKO mice could be attributed to lower dopamine uptake. In extracellular dopamine transients that were matched for peak  $[DA]_0$  ( $1.0 \pm 0.1 \mu\text{M}$ ), the decay rate was similar in each genotype (Fig. 5D). Because the decay phase of the dopamine transients is a function of dopamine uptake by DAT, this suggests that the rate of reuptake was not different in TKO mice compared with wild-type control mice.

#### Attenuated responses of TKO mice to psychostimulants

Our studies of TKO mice revealed a paradoxical combination of reduced striatal dopamine content but a hyperdopaminergic

phenotype associated with a greater realizability but unchanged reuptake of this neurotransmitter.

Additional data confirm that presynaptic dopamine stores are reduced in the striatum of mutant mice and also argue against a hypothesis of upregulation of postsynaptic transduction mechanisms rather than enhanced presynaptic dopamine releasability. We found that injection of 4 mg/kg dAMPH, which displaces dopamine stored in synaptic vesicles into extracellular space and whose effects depend on the size of presynaptic dopamine stores, but not regulated exocytosis, stimulated locomotor activity of TKO mice to a lesser and slower extent than of wild-type (Fig. 6*A,B*) or single-synuclein-KO mice (our unpublished data), whereas this activity was significantly greater in mutants when animals were first placed in a novel nonanxiogenic environment. In contrast, the locomotor response of TKO mice to injection of 10 mg/kg cocaine, which blocks dopamine uptake but does not induce reverse transport of dopamine from presynaptic terminal stores, was similar to wild-type mice (Fig. 6*C*). The difference in the effect of dAMPH and cocaine on TKO mice supports the hypothesis that dopaminergic presynaptic terminals of these mice have reduced levels of the neurotransmitter stored in synaptic vesicles. Notably, boosting of presynaptic dopamine storage by injection of 50 mg/kg methyl L-DOPA 20 min before placing animal in a novel nonanxiogenic environment did not change the behavior of TKO mice before amphetamine injection but restored the level of their dAMPH-induced locomotor activity to the level of wild-type mice (Fig. 6*B*).

Direct activation of postsynaptic D<sub>1</sub>/D<sub>2</sub> dopamine receptors by apomorphine (APO) shows that a transiently induced characteristic “climbing” behavior (Protais et al., 1976) was slightly less marked in TKO mice than in wild-type mice (Fig. 6*D*), suggesting that postsynaptic dopamine signaling is in fact modestly attenuated in the absence of synucleins, which is similar to other mouse lines with a hyperdopaminergic phenotypes and probably represent mechanisms in which downregulation of postsynaptic D<sub>1</sub>/D<sub>2</sub> heteroreceptors compensates for increased levels of dopamine in the synaptic cleft (Zhuang et al., 2001). This result further supports the hypothesis that presynaptic mechanisms are responsible for the hyperdopaminergic phenotype of TKO mice.

#### No gross ultrastructural changes of striatal dopaminergic axons in TKO mice

Quantitative electron-microscopic analyses of dopaminergic profiles in the dorsal striatum of TKO and wild-type mice performed on sections immunostained for TH using two techniques (Fig. 7*A,B*) indicated the overall density of TH-positive profiles, the number of mitochondria per structure and synaptic incidence, were not different between two genotypes. Analysis of all TH-immunogold profiles, as well as the subgroup forming syn-

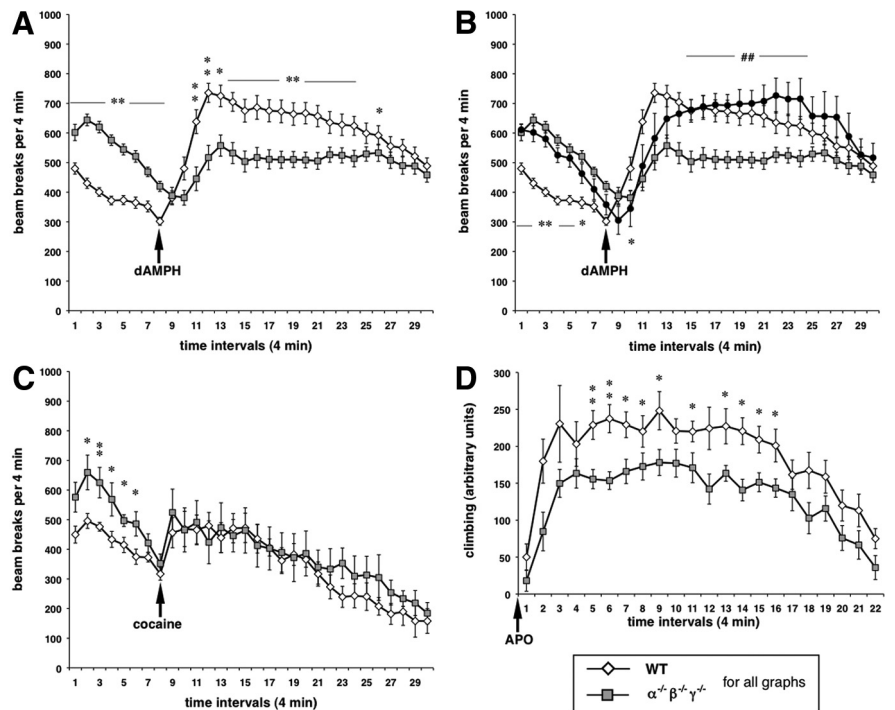


**Figure 6.** Behavior of wild-type and triple-synuclein-null mutant mice after pharmacological challenge of dopamine neurotransmission. The locomotor activity (*A–C*) or climbing behavior (*D*) of wild-type (WT) (white diamonds) and TKO ( $\alpha^{-/-}\beta^{-/-}\gamma^{-/-}$ ) (gray squares). *A*, Animals were injected with 4 mg/kg dAMPH after monitoring of their activity in novel environment (nonanxiogenic activity camera with infrared beams) for 30 min and returned to the same camera for an additional 90 min. Statistically significant increase in the locomotor activity of mutant mice before treatment and decrease after treatment was observed. *B*, A graph showing locomotor activity of triple-synuclein-null mutant mice pretreated with 50 mg/kg L-DOPA 20 min before placing in the activity camera and consequent injecting dAMPH (black circles) overlays the same graphs as in *A*. Statistically significant difference in the locomotor activity of wild-type and L-DOPA-pretreated mice (\*) or naive and L-DOPA-pretreated mutant mice (\*) is shown. *C*, The same protocol as described for *A* was used to assess locomotion of mice treated with 10 mg/kg cocaine. For all panels, statistically significant difference between two groups is shown for each 4 min interval (\*\*, ##  $p < 0.01$ ; \*  $p < 0.05$ ; Kolmogorov–Smirnov test). *D*, Scoring of climbing behavior of mice after injection with 4 mg/kg APO was performed as described in Materials and Methods.

aptic specializations, showed trends toward reduction in some parameters in TKO mice, such as the cross-sectional area of TH-positive profiles (18.6% smaller in all profiles; 35.6% smaller in synapse-forming profiles), the number of synaptic vesicles per profile (6.2 and 38.5% less), and also in the average distance of a synaptic vesicle from the plasma membrane (5.2 and 14.4% smaller) (Fig. 7*D*), but trends toward opposite outcomes in all versus synapse-forming structures for other parameters, for example, for the density of vesicles (9.5% increase across all versus 14.3% decrease in synapse-forming) and the average intervesicle distance, an indication of clustering [24.8% decrease (Fig. 7*C*) vs 3.0% increase]. In TH-immunogold profiles that formed synapses, the average distance of vesicles to the active zone was smaller in the mutant animals (22.4% decreased) (Fig. 7*D*). However, differences in these or other studied parameters [data are available (see Notes)] were not statistically significant, suggesting that the ultrastructure of dopaminergic synapses in the striatum is not substantially affected by the absence of synucleins.

#### Normal abundance of SNARE complexes in the dorsal striatum of TKO mice

Recent *in vivo* studies demonstrated that synucleins might regulate neurotransmitter release by regulating synaptic SNARE complex assembly and/or distribution of SNARE proteins within synapses (Chandra et al., 2005; Burré et al., 2010; Garcia-

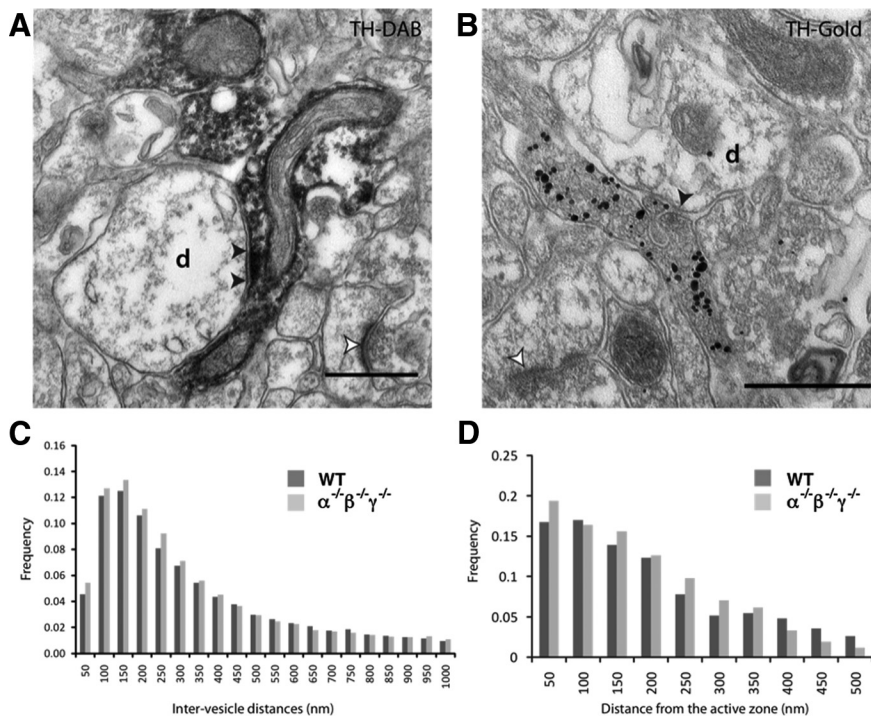


**Figure 7.** Electron-microscopic analyses of dopaminergic structures within the dorsal striatum in wild-type and triple-synuclein-null mutant mice. Electron micrographs of TH-immunoreactive synaptic boutons in the dorsolateral striatum of a TKO mouse. The immunoreactivity was revealed by the peroxidase method with diaminobenzidine as the chromogen (**A**) or the immunogold method (**B**). The bouton forms symmetrical synaptic contact (arrowheads) with a dendritic shaft (d). Note the nonimmunoreactive terminals forming an asymmetrical synaptic contact (white arrowheads) with a spine. Scale bars, 0.5  $\mu$ m. **C**, Frequency distribution of the intervesicle distances in immunogold-labeled TH-positive structures (150 TH-immunoreactive profiles from 3 animals per genotype). **D**, Frequency distribution of the distances of vesicles from the active zone in immunogold-labeled TH-positive profiles that formed synaptic specializations (23 TH-immunoreactive synaptic boutons from 3 animals per genotype).

Reitböck et al., 2010). Analysis of total brain lysates revealed attenuated assembly of SNARE complexes in TKO mice, which was mirrored by a positive effect of  $\alpha$ -synuclein overexpression on this process in cultured hippocampal neurons (Burré et al., 2010). In contrast, accumulation of  $\alpha$ -synuclein in striatal dopaminergic terminals of transgenic mice resulted in reduced dopamine release (Garcia-Reitböck et al., 2010). Overall, no uniform pattern emerges from these studies, suggesting that different types of synapses may respond differently to changes in synucleins availability. To reveal whether the absence of synucleins affects SNARE complex assembly in the dorsal striatum, we quantified the amount of vSNARE (vesicular SNARE) VAMP2/synaptobrevin coimmunoprecipitated with tSNARE (target membrane-associated SNARE) SNAP-25 from the lysates of freshly dissected dorsal striatum tissue and found no difference between wild-type and TKO animals (Fig. 8). We also observed no changes in distribution of SNAP-25 or CSP, a cochaperone of SNARE complex assembly, in the striatum of TKO mice [data are available (see Notes)].

## Discussion

The presynaptic functions of synucleins have been intensively explored in many neuron types, including in recent studies using TKO mice (Burré et al., 2010; Gretchen-Harrison et al., 2010), but surprisingly, their functions at dopamine release sites have remained poorly defined. Yet it may be imperative to understand synuclein biology within dopaminergic neurons if we are to learn how synuclein pathology is associated with the preferential degeneration of these neurons in PD. Here, we show that deletion of

all three members of the synuclein family significantly modifies the function of some mesostriatal dopaminergic systems but not others. Dopamine release from dorsal striatal axons was greater in the absence of synucleins, and TKO mice exhibited hyperdopamine-like behaviors, despite lower dopamine content and no detectable disturbances in dopamine synthesis, neuron number, availability of vesicles, or SNARE complex formation. Furthermore, the neurochemical changes in dopaminergic synapse function were not detected in ventral striatum, indicating that synucleins differently govern dopamine transmission in nigrostriatal compared with mesolimbic neurons. These data suggest that synucleins limit vesicular dopamine transmission through mechanisms that differ from those reported in other neurons and, furthermore, reveal key differences that vary with dopaminergic neuron subtype.

## Modifications to presynaptic dopamine neurochemistry but not structure

Dopaminergic neurons in wild-type mice express all three members of the synuclein family. Data drawn from across our study indicate that many aspects of mesostriatal dopaminergic neuron biology do not differ between TKO and wild-type mice. We show normal numbers of dopaminergic neurons in SNpc and VTA, normal striatal abundance and distribution of specific proteins markers, and no difference in the ultrastructure of dopaminergic synapses or vesicle distribution.

By contrast, our analysis of dopamine neurochemistry and transmission as well as our behavioral analysis revealed significant effects of synuclein depletion on mesostriatal function. Despite normal level of TH activity, dopamine content was  $\sim$ 40% lower in dorsal striatum of TKO than wild-type mice, a deficit much more marked than reported for double- $\alpha/\beta$ -synuclein-KO mice (Chandra et al., 2004) or a line of  $\alpha$ -synuclein-KO mice on a mixed genetic background (Abeliovich et al., 2000). No deficit was detected in double- $\alpha/\gamma$ -synuclein-KO (Robertson et al., 2004; Senior et al., 2008) or  $\beta/\gamma$ -synuclein-KO mice (our unpublished data) on a pure C57BL/6J genetic background, and only in aged ( $\geq$  2 years)  $\alpha$ -synuclein-KO mice does striatal dopamine content decline to a level comparable with that seen here in adult TKO mice (Al-Wandi et al., 2010). These observations indicate that all three synucleins are involved in dopamine regulation and that, although elimination of each family member can be at least partially or temporarily compensated for, loss of all three synucleins results in the greatest reduction in the capacity of synapses to store dopamine. In conjunction with our EM data that vesicle number is not modified, the reduced tissue dopamine content suggests that, in TKO mice, less dopamine is stored per vesicle.

The levels of dopamine metabolites DOPAC and HVA in TKO mice were reduced to a lesser extent than dopamine, resulting in higher metabolite/dopamine ratios. This ratio is often used to indicate that a greater percentage of dopamine is turned over

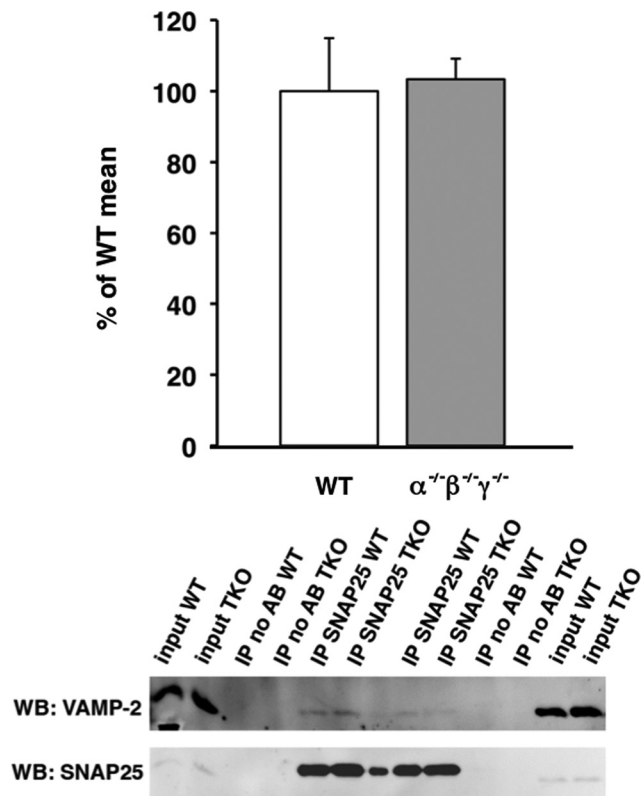


**Figure 8.** Quantification of SNARE complexes in the dorsal striatum of wild-type and triple-synuclein-null mutant mice. Coimmunoprecipitation of VAMP2/synaptobrevin with SNAP-25 was used to assess the abundance of SNARE complexes in the dorsal striatum of wild-type (WT) and TKO ( $\alpha^{-/-}\beta^{-/-}\gamma^{-/-}$ ) mice. The bar chart shows amount of VAMP2/synaptobrevin in SNAP-25 immunoprecipitates normalized to the amount of precipitated SNAP-25 and expressed as percentage of mean amount WT samples ( $\pm$  SEM; results of 3 independent experiments; 3 WT and 3 TKO mice used in each of these experiments). A representative Western blot shows results of analysis of two independent pairs of WT and TKO mice.

or, in other words, is released from vesicular stores with access to extracellular and cytosolic metabolic pathways. Indeed, direct study of dopamine release using FCV revealed a striking elevation of the releasability of dopamine in the striatum in TKO mice. This increase was not caused by a reduction in dopamine uptake rate, an upregulation of nicotinic acetylcholine receptor function, or by increased sensitivity of the presynaptic exocytotic machinery to calcium or increased dopamine release probability [as determined by measurements of frequency sensitivity, which should be inversely correlated with release probability (Rice and Cragg, 2004)]. Rather, the data suggest a generalized increase in dopamine releasability per stimulus. Behavioral tests also suggested that TKO mice had increased rather than decreased levels of striatal dopamine. Furthermore, the experiments with a dopamine-releasing agent (amphetamine) and a receptor ligand (apomorphine) were in agreement with enhanced presynaptic dopamine release despite reduced dopamine storage, and not with any additional apparent upregulation of postsynaptic receptor number or efficacy.

Several mechanisms, which are not mutually exclusive, can underlie enhanced releasability from presynaptic terminals with diminished content of the neurotransmitter. For example, neurotransmitter releasability can be elevated if the recycling, readily releasable pool of these vesicles is increased at the expense of the reserve pool. Increased expression of  $\alpha$ -synuclein in cultured hippocampal neurons reduces the size of the recycling pool and

can thus inhibit synaptic vesicle exocytosis (Nemani et al., 2010; Scott et al., 2010). However, striatal dopaminergic synapses are morphologically and functionally distinct from these synapses: they lack spatially defined clusters of reserve and recycling vesicles. Our ultrastructural analyses indicated that the presynaptic distribution of synaptic vesicles in dorsal striatum is not modified in TKO mice, suggesting that synucleins do not regulate the overall anatomical distribution of vesicles within dopaminergic axons, unlike in other axon types, and that this does not explain a change in dopamine releasability in TKO mice.

Another possible explanation for enhanced neurotransmitter releasability is increased rate of vesicle fusion. However, such an assumption is inconsistent with the recently obtained evidence that in hippocampal neurons  $\alpha$ -synuclein promotes activity-dependent assembly of SNARE complexes (Chandra et al., 2005; Burré et al., 2010), which is a crucial step in the vesicle fusion cycle. Moreover, we demonstrate here that, in dorsal striatum, the abundance of SNARE complexes is not different in TKO and wild-type mice. Therefore, it is unlikely that increased releasability of dopamine in the absence of synucleins is caused by modified levels of SNARE complexes with consequent acceleration of vesicle fusion.

It remains feasible that the presence or absence of synucleins might affect formation of a fusion pore and thus the fate of a fused vesicle (i.e., kiss-and-run or full-collapse fusion with the presynaptic plasma membrane). A boost in dopamine release could thus arise from the release of a greater proportion of contents of each vesicle or the number of dopamine quanta released per stimulus. Additional detailed studies are required to test this hypothesis and understand whether and why any of these mechanisms differ in nigrostriatal compared with mesolimbic neurons. We cannot entirely exclude the possibility that changes to dopamine release in the absence of synucleins reflect consequences of the developmental compensation of the nigrostriatal neurons for the absence of synucleins.

These data together suggest that, in the absence of synucleins, dopamine axons release more vesicles (or more content of each vesicle), each of which has a decreased dopamine load. The most parsimonious explanation for reduced dopamine content of each vesicle could be a downregulation in response to a gain in releasability: indeed content is lower when extracellular availability of dopamine is increased in other models (e.g., DAT-KO mice) (Jones et al., 1998). However, differences in dopamine releasability have been reported without complementary reductions in dopamine content in striatal terminals of  $\alpha/\gamma$ -synuclein double-KO mice (Senior et al., 2008). Therefore, it is feasible that multiple synuclein-dependent mechanisms might differently upregulate releasability on the one hand and disrupt dopamine storage on the other (e.g., compromise VMAT2 function, which in turn downregulates dopamine content).

#### Regionally distinct effects of synuclein deletion: nigrostriatal versus mesolimbic dopamine synapses

It is striking that synuclein depletion affects presynaptic dopamine neurochemistry only in dorsal and not ventral striatum. Thus, the roles of synucleins that we have described here in dopaminergic neurons may differ substantially between neurons of different neurotransmitter type (e.g., dopaminergic vs hippocampal glutamatergic neurons) and, moreover, may be specific to neuron subtype even for a given transmitter. Furthermore, since dopaminergic neurons innervating the dorsal striatum (nigrostriatal pathway) degenerate in preference to those innervating the ventral striatum (mesolimbic pathway) in PD, our finding may offer signif-

icant new insight into the preferential degeneration seen in PD. Although striking, the finding that a mechanism regulating dopamine neurotransmission might differ in nigrostriatal versus mesolimbic neurons is not entirely unsurprising. A large body of work suggests that nigrostriatal neurons differ from mesolimbic neurons in many features [e.g., embryonic source and stage of ontogenetic development, neuroanatomy of projections and inputs, proteins expression levels including dopamine cell markers (DAT, VMAT2, D<sub>2</sub> receptors), ion channels and other proteins, influence of neuromodulatory receptors as well as the regulation of dopamine release probability and their susceptibility to neurodegeneration (for review, see Korotkova et al., 2004; Björklund and Dunnett, 2007; Liss and Roeper, 2008)]. Synuclein function may be another key feature that variably influences the function of nigrostriatal versus mesolimbic neurons.

## Conclusions

These data significantly revise our understanding of synuclein function. They indicate that synucleins in some dopaminergic neurons limit synaptic neurotransmission through mechanisms that differ from those reported in other neurons, which have included vesicle pool redistribution or SNARE complex formation. These data shed light on the distinct role of synucleins in dopaminergic neurons and reveal type-specific differences between dopaminergic neurons, which may ultimately offer insight into the preferential degeneration of neurons subsets in PD.

## Notes

Supplemental Figures S1–S5 and Supplemental Tables 1–4 for this article are available at <https://docs.google.com/viewer?a=v&pid=explorer&chrome=true&srcid=0B-2G31EgcACfZrjZDFjZTtNGRIZi00ODI2LTg2NWU0OWYyZ4YzA2OGUx&hl=en>. This material has not been peer reviewed.

## References

- Abeliovich A, Schmitz Y, Fariñas I, Choi-Lundberg D, Ho WH, Castillo PE, Shinsky N, Verdugo JM, Armanini M, Ryan A, Hynes M, Phillips H, Sulzer D, Rosenthal A (2000) Mice lacking alpha-synuclein display functional deficits in the nigrostriatal dopamine system. *Neuron* 25:239–252.
- Al-Wandi A, Ninkina N, Millership S, Williamson SJ, Jones PA, Buchman VL (2010) Absence of alpha-synuclein affects dopamine metabolism and synaptic markers in the striatum of aging mice. *Neurobiol Aging* 31:796–804.
- Björklund A, Dunnett SB (2007) Dopamine neuron systems in the brain: an update. *Trends Neurosci* 30:194–202.
- Buchman VL, Hunter HJ, Pinón LG, Thompson J, Privalova EM, Ninkina NN, Davies AM (1998) Persyn, a member of the synuclein family, has a distinct pattern of expression in the developing nervous system. *J Neurosci* 18:9335–9341.
- Burré J, Sharma M, Tsetsenis T, Buchman V, Etherton MR, Südhof TC (2010) Alpha-synuclein promotes SNARE-complex assembly in vivo and in vitro. *Science* 329:1663–1667.
- Cabin DE, Shimazu K, Murphy D, Cole NB, Gottschalk W, McIlwain KL, Orrison B, Chen A, Ellis CE, Paylor R, Lu B, Nussbaum RL (2002) Synaptic vesicle depletion correlates with attenuated synaptic responses to prolonged repetitive stimulation in mice lacking alpha-synuclein. *J Neurosci* 22:8797–8807.
- Carlsson A, Davis JN, Kehr W, Lindqvist M, Atack CV (1972) Simultaneous measurement of tyrosine and tryptophan hydroxylase activities in brain in vivo using an inhibitor of the aromatic amino acid decarboxylase. *Naunyn-Schmiedeberg's Arch Pharmacol* 275:153–168.
- Chandra S, Fornai F, Kwon HB, Yazdani U, Atasoy D, Liu X, Hammer RE, Battaglia G, German DC, Castillo PE, Südhof TC (2004) Double-knockout mice for alpha- and beta-synucleins: effect on synaptic functions. *Proc Natl Acad Sci U S A* 101:14966–14971.
- Chandra S, Gallardo G, Fernández-Chacón R, Schlüter OM, Südhof TC (2005) Alpha-synuclein cooperates with CSPalpha in preventing neurodegeneration. *Cell* 123:383–396.
- Cragg SJ (2003) Variable dopamine release probability and short-term plasticity between functional domains of the primate striatum. *J Neurosci* 23:4378–4385.
- Cragg SJ, Hille CJ, Greenfield SA (2000) Dopamine release and uptake dynamics within nonhuman primate striatum *in vitro*. *J Neurosci* 20:8209–8217.
- Exley R, Clements MA, Hartung H, McIntosh JM, Cragg SJ (2008) Alpha6-containing nicotinic acetylcholine receptors dominate the nicotine control of dopamine neurotransmission in nucleus accumbens. *Neuropsychopharmacology* 33:2158–2166.
- Fountaine TM, Venda LL, Warrick N, Christian HC, Brundin P, Channon KM, Wade-Martins R (2008) The effect of alpha-synuclein knockdown on MPP+ toxicity in models of human neurons. *Eur J Neurosci* 28:2459–2473.
- Garcia-Reitböck P, Anichtchik O, Bellucci A, Iovino M, Ballini C, Fineberg E, Ghetti B, Della Corte L, Spano P, Tofaris GK, Goedert M, Spillantini MG (2010) SNARE protein redistribution and synaptic failure in a transgenic mouse model of Parkinson's disease. *Brain* 133:2032–2044.
- Giros B, Jaber M, Jones SR, Wightman RM, Caron MG (1996) Hyperlocomotion and indifference to cocaine and amphetamine in mice lacking the dopamine transporter. *Nature* 379:606–612.
- Goedert M (2001) Alpha-synuclein and neurodegenerative diseases. *Nat Rev Neurosci* 2:492–501.
- Greten-Harrison B, Polydoro M, Morimoto-Tomita M, Diao L, Williams AM, Nie EH, Makani S, Tian N, Castillo PE, Buchman VL, Chandra SS (2010) alpha-beta-gamma-Synuclein triple knockout mice reveal age-dependent neuronal dysfunction. *Proc Natl Acad Sci U S A* 107:19573–19578.
- Jenco JM, Rawlingson A, Daniels B, Morris AJ (1998) Regulation of phospholipase D2: selective inhibition of mammalian phospholipase D isoenzymes by alpha- and beta-synucleins. *Biochemistry* 37:4901–4909.
- Jones SR, Gainetdinov RR, Jaber M, Giros B, Wightman RM, Caron MG (1998) Profound neuronal plasticity in response to inactivation of the dopamine transporter. *Proc Natl Acad Sci U S A* 95:4029–4034.
- Korotkova TM, Ponomarenko AA, Brown RE, Haas HL (2004) Functional diversity of ventral midbrain dopamine and GABAergic neurons. *Mol Neurobiol* 29:243–259.
- Larsen KE, Schmitz Y, Troyer MD, Mosharov E, Dietrich P, Quazi AZ, Savalle M, Nemani V, Chaudhry FA, Edwards RH, Stefanis L, Sulzer D (2006) alpha-Synuclein overexpression in PC12 and chromaffin cells impairs catecholamine release by interfering with a late step in exocytosis. *J Neurosci* 26:11915–11922.
- Larsson M, Broman J (2005) Different basal levels of CaMKII phosphorylated at Thr286/287 at nociceptive and low-threshold primary afferent synapses. *Eur J Neurosci* 21:2445–2458.
- Lee FJ, Liu F, Pristupa ZB, Niznik HB (2001) Direct binding and functional coupling of alpha-synuclein to the dopamine transporters accelerate dopamine-induced apoptosis. *FASEB J* 15:916–926.
- Liss B, Roeper J (2008) Individual dopamine midbrain neurons: functional diversity and flexibility in health and disease. *Brain Res Rev* 58:314–321.
- Liu D, Jin L, Wang H, Zhao C, Duan C, Lu L, Wu B, Yu S, Chan P, Li Y, Yang H (2008) Silencing alpha-synuclein gene expression enhances tyrosine hydroxylase activity in MN9D cells. *Neurochem Res* 33:1401–1409.
- Liu S, Ninan I, Antonova I, Battaglia F, Trinchese F, Narasanna A, Kolidilov N, Dauer W, Hawkins RD, Arancio O (2004) alpha-Synuclein produces a long-lasting increase in neurotransmitter release. *EMBO J* 23:4506–4516.
- Mizuta I, Tsunoda T, Satake W, Nakabayashi Y, Watanabe M, Takeda A, Hasegawa K, Nakashima K, Yamamoto M, Hattori N, Murata M, Toda T (2008) Calbindin 1, fibroblast growth factor 20, and alpha-synuclein in sporadic Parkinson's disease. *Hum Genet* 124:89–94.
- Moss J, Bolam JP (2008) A dopaminergic axon lattice in the striatum and its relationship with cortical and thalamic terminals. *J Neurosci* 28:11221–11230.
- Nemani VM, Lu W, Berge V, Nakamura K, Onoa B, Lee MK, Chaudhry FA, Nicoll RA, Edwards RH (2010) Increased expression of alpha-synuclein reduces neurotransmitter release by inhibiting synaptic vesicle re-clustering after endocytosis. *Neuron* 65:66–79.
- Ninkina N, Papachroni K, Robertson DC, Schmidt O, Delaney L, O'Neill F, Court F, Rosenthal A, Fleetwood-Walker SM, Davies AM, Buchman VL

- (2003) Neurons expressing the highest levels of gamma-synuclein are unaffected by targeted inactivation of the gene. *Mol Cell Biol* 23:8233–8245.
- Ninkina N, Peters O, Millership S, Salem H, van der Putten H, Buchman VL (2009) Gamma-synucleinopathy: neurodegeneration associated with overexpression of the mouse protein. *Hum Mol Genet* 18:1779–1794.
- Pankratz N, Wilk JB, Latourelle JC, DeStefano AL, Halter C, Pugh EW, Doheny KF, Gusella JF, Nichols WC, Foroud T, Myers RH (2009) Genomewide association study for susceptibility genes contributing to familial Parkinson disease. *Hum Genet* 124:593–605.
- Peng X, Tehranian R, Dietrich P, Stefanis L, Perez RG (2005) Alpha-synuclein activation of protein phosphatase 2A reduces tyrosine hydroxylase phosphorylation in dopaminergic cells. *J Cell Sci* 118:3523–3530.
- Perez RG, Waymire JC, Lin E, Liu JJ, Guo F, Zigmond MJ (2002) A role for  $\alpha$ -synuclein in the regulation of dopamine biosynthesis. *J Neurosci* 22:3090–3099.
- Protais P, Costentin J, Schwartz JC (1976) Climbing behavior induced by apomorphine in mice: a simple test for the study of dopamine receptors in striatum. *Psychopharmacology (Berl)* 50:1–6.
- Rice ME, Cragg SJ (2004) Nicotine amplifies reward-related dopamine signals in striatum. *Nat Neurosci* 7:583–584.
- Robertson DC, Schmidt O, Ninkina N, Jones PA, Sharkey J, Buchman VL (2004) Developmental loss and resistance to MPTP toxicity of dopaminergic neurons in substantia nigra pars compacta of gamma-synuclein, alpha-synuclein and double alpha/gamma-synuclein null mutant mice. *J Neurochem* 89:1126–1136.
- Satake W, Nakabayashi Y, Mizuta I, Hirota Y, Ito C, Kubo M, Kawaguchi T, Tsunoda T, Watanabe M, Takeda A, Tomiyama H, Nakashima K, Hasegawa K, Obata F, Yoshikawa T, Kawakami H, Sakoda S, Yamamoto M, Hattori N, Murata M, et al. (2009) Genome-wide association study identifies common variants at four loci as genetic risk factors for Parkinson's disease. *Nat Genet* 41:1303–1307.
- Scholz SW, Houlden H, Schulte C, Sharma M, Li A, Berg D, Melchers A, Paudel R, Gibbs JR, Simon-Sanchez J, Paisan-Ruiz C, Bras J, Ding J, Chen H, Traynor BJ, Arepalli S, Zonozi RR, Revesz T, Holton J, Wood N, et al. (2009) SNCA variants are associated with increased risk for multiple system atrophy. *Ann Neurol* 65:610–614.
- Scott DA, Tabarean I, Tang Y, Cartier A, Masliah E, Roy S (2010) A pathologic cascade leading to synaptic dysfunction in  $\alpha$ -synuclein-induced neurodegeneration. *J Neurosci* 30:8083–8095.
- Senior SL, Ninkina N, Deacon R, Bannerman D, Buchman VL, Cragg SJ, Wade-Martins R (2008) Increased striatal dopamine release and hyperdopaminergic-like behaviour in mice lacking both alpha-synuclein and gamma-synuclein. *Eur J Neurosci* 27:947–957.
- Simón-Sánchez J, Schulte C, Bras JM, Sharma M, Gibbs JR, Berg D, Paisan-Ruiz C, Lichtner P, Scholz SW, Hernandez DG, Krüger R, Federoff M, Klein C, Goate A, Perlmutter J, Bonin M, Nalls MA, Illig T, Gieger C, Houlden H, et al. (2009) Genome-wide association study reveals genetic risk underlying Parkinson's disease. *Nat Genet* 41:1308–1312.
- Tehrani R, Montoya SE, Van Laar AD, Hastings TG, Perez RG (2006) Alpha-synuclein inhibits aromatic amino acid decarboxylase activity in dopaminergic cells. *J Neurochem* 99:1188–1196.
- Trojanowski JQ, Lee VM (2002) Parkinson's disease and related synucleinopathies are a new class of nervous system amyloidoses. *Neurotoxicology* 23:457–460.
- Unger EL, Eve DJ, Perez XA, Reichenbach DK, Xu Y, Lee MK, Andrews AM (2006) Locomotor hyperactivity and alterations in dopamine neurotransmission are associated with overexpression of A53T mutant human alpha-synuclein in mice. *Neurobiol Dis* 21:431–443.
- Venda LL, Cragg SJ, Buchman VL, Wade-Martins R (2010) alpha-Synuclein and dopamine at the crossroads of Parkinson's disease. *Trends Neurosci* 33:559–568.
- Wersinger C, Sidhu A (2003) Attenuation of dopamine transporter activity by alpha-synuclein. *Neurosci Lett* 340:189–192.
- Yavich L, Tanila H, Vepsäläinen S, Jäkälä P (2004) Role of  $\alpha$ -synuclein in presynaptic dopamine recruitment. *J Neurosci* 24:11165–11170.
- Yavich L, Oksman M, Tanila H, Kerokoski P, Hiltunen M, van Groen T, Puolivali J, Männistö PT, García-Horsman A, MacDonald E, Beyreuther K, Hartmann T, Jäkälä P (2005) Locomotor activity and evoked dopamine release are reduced in mice overexpressing A30P-mutated human alpha-synuclein. *Neurobiol Dis* 20:303–313.
- Zhuang X, Oosting RS, Jones SR, Gainetdinov RR, Miller GW, Caron MG, Hen R (2001) Hyperactivity and impaired response habituation in hyperdopaminergic mice. *Proc Natl Acad Sci U S A* 98:1982–1987.